Dynamic Acquisition with a Three-Headed SPECT System: Application to Technetium 99m-SQ30217 Myocardial Imaging

Kenichi Nakajima, Junichi Taki, Hisashi Bunko, Masamichi Matsudaira, Akira Muramori, Ichiro Matsunari, Kinichi Hisada, and Takashi Ichihara

Department of Nuclear Medicine and Division of Radioisotopes, Kanazawa University Hospital, Kanazawa, Japan and Toshiba Nasu Works, Tochigi, Japan

A method for SPECT data acquisition, "continuous repetitive rotation acquisition," was developed with a high-sensitivity three-headed SPECT system. The method was applied to the dynamic imaging of ^{99m}Tc-SQ30217, a new myocardial imaging agent. After acquisition and reconstruction of SPECT data every minute, projection images at arbitrary intervals were used for tomographic reconstruction to determine the best timing of SPECT imaging in ^{99m}Tc-SQ30217. Based on a comparison of several possible acquisition intervals, SPECT data acquisition within 9 min after injection is recommended because of high myocardial uptake (myocardium-to-lung ratio, 2.83 ± 0.42 (mean ± s.e.m.) at 3–6 min) and relatively low hepatic uptake (myocardium-to-liver ratio, 0.85 ± 0.13 at 3–6 min). The rate constant of the clearance of ^{99m}Tc-SQ30217 from the myocardium obtained by SPECT was: $k_1 = 0.249 \pm 0.050$ per min (average half-life = 2.8 min) and $k_2 = 0.012 \pm 0.004$/min (average half-life = 58 min). The continuous repetitive rotation acquisition SPECT study appears useful for imaging SQ30217 with its rapidly changing myocardial distribution.

J Nucl Med 1991; 32:1273–1277

Considerable attention has been paid to the ^{99m}Tc-labeled myocardial perfusion imaging agents that may replace the ^{201}Tl in clinical cardiology (*1*). One new technetium imaging agent, chloro(methylboron (1-)-tris(1,2-cyclohexanedionedioxime) N,N′,N″,N‴,N⁗,N⁗′) (SQ30217) has been reported to be a promising perfusion imaging agent with high myocardial uptake comparable to that of ^{201}Tl (*2–8*). Animal experiments and clinical trials have indicated that SQ30217 is an effective myocardial imaging agent (*3–13*). However, despite the high accumulation in the myocardium, rapid clearance from the myocardium and relatively high accumulation in the liver place vigorous requirements on imaging patients with this agent (*9–12*), particularly when single-photon emission computed tomography (SPECT) is desired. Although the application of SPECT in ^{201}Tl myocardial scintigraphy has become a routine diagnostic method, the high sensitivity SPECT system in which rapid data acquisition is possible, is appropriate for radiopharmaceuticals showing rapid clearance such as SQ30217. One technical solution is the use of a three-headed SPECT system, in which both high sensitivity and high resolution have been achieved (*14–18*).

The objectives of this study were (1) evaluation of a method of data acquisition and processing (i.e., continuous repetitive data sampling method) and a method for editing the SPECT images at arbitrary intervals and (2) determination of the best timing of data acquisition using this radiopharmaceutical.

MATERIALS AND METHODS

SPECT System

The photon detecting system consisted of three scinticameras (GCA 9300A, Toshiba, Tokyo, Japan), which surrounds the imaging field triangularly (*16*). Each camera has a rectangular field of view (the effective field of view is 38 × 21 cm), and the radius of rotation was adjusted by radial translation. Data were recorded with a general-purpose (GP) collimator for this dynamic study. The detector system was interfaced to a dedicated nuclear medicine computer (GMS 550U, Toshiba). The sensitivity measured with GP collimator was 2.13K cps/μCi/ml/cm for 1-cm slice thickness. The FWHM value was measured with 128 × 128 matrix and 90 projection data (4° step) was 16.9 mm with a general purpose collimator at the center of rotation with a radius of 20 cm. Data were acquired with continuous rotation (see below). The minimum time for a continuous rotation is 10 sec for body SPECT.

Subjects

The study group consisted of six patients suspected of ischemic heart disease. The definitive diagnosis was made in all patients by the clinical history, electrocardiography, coronary arteriography within a month of the ^{99m}Tc-SQ30217 study and ^{201}Tl scintigraphy. All the SPECT studies with ^{99m}Tc-SQ30217 were

Received Jun. 1, 1990; revision accepted Nov. 29, 1990.
For reprints contact: Kenichi Nakajima, MD, Department of Nuclear Medicine, Kanazawa University Hospital, 13-1 Takaramachi, Kanazawa, 920 Japan.

performed in the resting state. Table 1 summarizes the clinical data and the imaging results in these patients.

Preparation of ^{99m}Tc-SQ30217

The radiopharmaceutical was supplied in kit form (Squibb Japan, Tokyo). From 800 to 2000 MBq of ^{99m}Tc in 1 ml of 0.9% NaCl was added to the vial. The vial then was placed in a 100°C heating block for 15 min. After cooling the vial at room temperature, from 555 to 925 MBq (15–25 mCi) of ^{99m}Tc-SQ30217 was intravenously injected in each patient.

The labeling efficiency was measured with paper chromatography, and the percentage of free pertechnetate and reduced hydrolyzed technetium was monitored based on the method described by Narra et al. (7). The average labeling efficiency was 91% ± 2.3% (s.e.m.).

SPECT Data Acquisition

Dynamic data acquisition was performed with continuous rotation; images were recorded at 4° intervals in 64 × 64 matrices. The camera rotation of 120° around the chest in 60 sec covered the projections over 360°. The detectors were alternately and repeatedly rotated in clockwise and counterclockwise directions in a circular orbit. A total of 30 series of projection data (one per minute) acquired during a 30-min period were stored in the magnetic disc. A total of 2700 images were stored in each study (90 raw projection images).

Image Processing

To reconstruct transaxial images from the dynamic acquisition data, Butterworth and Ramp filters were employed. The parameter of the Butterworth filter was order 8, and the cutoff frequency was 0.25–0.30 cycle/pixel, depending on the image quality. Serial transaxial images were reconstructed with 2-pixel thickness (12.8 mm) in 8 slices using 360° projection data. After surveying all of the transaxial images, several appropriate ranges of acquisition duration were selected for further processing. Except for the first interval (from 0–1 min), which was not accepted because of the artifact during the initial passage of the tracer, arbitrary intervals could be chosen after 2 min. The raw projection images of the same projection direction were added at these pre-determined intervals. The Butterworth and Ramp filters were used to reconstruct transaxial images of a pixel thickness (6.4 mm). Vertical long-axis images and short-axis images were also generated. No attenuation correction was performed.

Data Analysis

The image quality and perfusion defect detection were visually compared among the reconstructed images made from several selected intervals. Time-activity curves (TACs) were generated using transaxial images at the mid-portion of the heart. Regions of interest (ROIs) were drawn over the myocardium and lungs without perfusion abnormalities. A ROI was also placed on the liver using the slice in which both the liver and inferior wall were visible. All SPECT counts were expressed as the percentage of the myocardial count at the second frame (1–2 min) normalized for variation of the injected dose, relative organ uptake, and patient stature.

After excluding the first datapoint from the TAC, non-linear least squares fitting was performed assuming multi-exponential function. Gauss-Newton's method with a weighting factor of 1 was used. Bi-exponential function:

$$\text{Count} = C_1 \exp(-k_1 t) + C_2 \exp(-k_2 t),$$

where C_1 and C_2 represent the relative counts of each exponential function at time $t = 0$, and k_1 and k_2 are the rate constants, best fit the clearance curve. In all the patients, the coefficients C_1 and C_2 and the rate constants k_1 and k_2 were calculated.

All results of relative SPECT count and ratios between the ROIs were expressed as mean ± s.e.m.

RESULTS

Figure 1 shows the serial changes of the distribution of ^{99m}Tc-SQ30217 in four transaxial slices. The first row acquired from 0 to 1 min had artifacts caused by the rapidly changing distribution of tracer during its first transit. In the second row (1–2 min), the artifact was negligible and a high myocardial uptake and relatively high lung activity, where the dorsal part of the lung had higher activity, were demonstrated. From 3 to 10 min, the myocardium was clearly visible, but the activity rapidly decreased with time. The clearance from the lung was also very rapid. In contrast, the hepatic activity rapidly increased. Observing the density in the lower section of the heart where both the liver and myocardium were visualized, the count density of the liver exceeded that of the myocardium after 3 or 4 min. In this patient, four successive short-axis slices from the mid-ventricular portion to the apex are shown in Figure 2. The SPECT images were reconstructed from the added projection data from 3 to 6 min, 6 to 9 min, 9 to 12 min, and 11 to 21 min. The patient had total occlusion of the circumflex branch of the

TABLE 1
Study Group and the Results of ^{201}Tl and ^{99m}Tc-SQ30217 Studies

Case no.	Age	Sex	Clinical diagnosis	Coronary arteriography	^{201}Tl		^{99m}Tc-SQ defect	
					Ex/Rest	defect	RD	at rest
1	69	M	OMI, AP	2VD (LAD, LCX)	Ex	inferolateral	(+)	inferolateral
2	63	M	OMI, AP	3VD	Rest	anteroseptal		anteroseptal
3	54	M	OMI	1VD (LAD)	Ex	anterior	(−)	anterior
4	39	M	DM, FH	n.s.	Ex	no		no
5	65	M	OMI	3VD	Ex	inferior	(−)	inferior
6	69	F	AP	n.s.	Ex	no		no

AP = angina pectoris; OMI = old myocardial infarction; DM = diabetes mellitus; FH = familial hypercholesterolemia; VD = vessel disease; LAD = left anterior descending artery; LCX = left circumflex artery; RD = redistribution; and n.s. = no significant stenosis (≤50%).

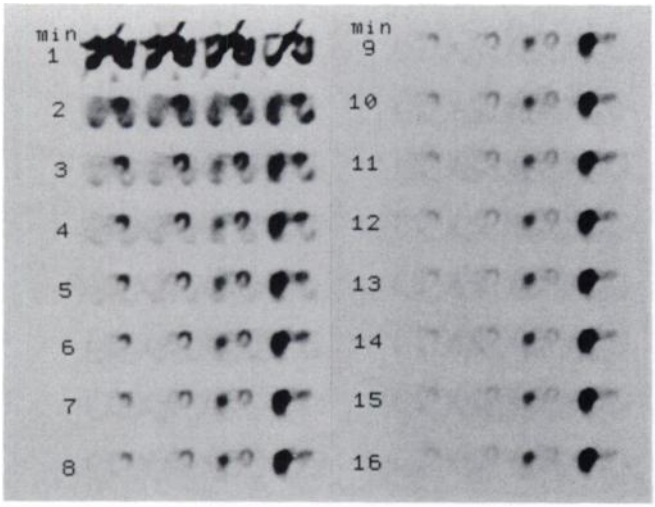

FIGURE 1. Serial changes of the accumulation pattern in the first 16 min in four transaxial slices. In each row, the SPECT acquisition was performed in 1 min with the continuous rotation mode.

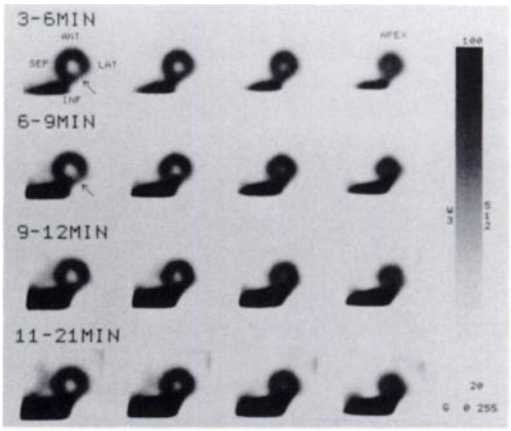

FIGURE 2. Comparison of the timing of data acquisition using 3–6, 6–9, 9–12 and 11–21 min. Short-axis images acquired for 3 min within 9 min after injection demonstrated reduced perfusion in the inferolateral wall as indicated by the arrows, while hepatic activity superimposed on the inferoapical wall after 9 min.

left coronary artery, and an inferolateral perfusion defect was observed on exercise ^{201}Tl scintigraphy. The inferolateral segment showed partial redistribution in the 3-hr image and significant redistribution in the 24-hr image. In the ^{99m}Tc-SQ30217 images, decreased inferolateral activity was clearly separated from the hepatic activity in the 3–6-min and 6–9-min images, while the inferior wall of the 9–12-min and 11–21-min images was obscured by the hepatic accumulation.

Table 2 shows relative SPECT count densities in the myocardium, lung, liver, and the ratios among them which were calculated in the same intervals as in Figure 2 (n = 6). The SPECT count in the first frame was excluded from the analysis, because it contained the initial blood activity in the ventricular cavity and artifacts. The myocardial count rate in the 3–6-min image was 1.8 times higher than that of the 11–21-min image. The actual myocardial count density in the 3-min SPECT image from 3 to 6 min had 54% [(70% count/pixel/min × 3 min)/(39% count/pixel/min × 10 min)] of the counts obtained from the 10-min image from 11 to 21 min. The ratio of myocardium to lung was about 2.8 within 9 min, but slightly decreased after 10 min. The myocardium-to-liver ratio was the highest in the 1-2-min image. If 3-min data were used to reduce the statistical noise, the myocardium-to-liver ratio was 0.85 in the 3–6-min image, while in the 11–21-min image the ratio dropped to 0.35.

Figure 3 shows the time-activity curves on the myocardium, lung, and liver. The SPECT count is standardized to a percentage of count/pixel/min as in Table 2. The lung activity decreased more rapidly than the myocardial activity. The hepatic activity increased rapidly, reached a peak at around 10–15 min, and gradually decreased thereafter. Large standard error of the hepatic activity was due to the variability of liver position at the level of lower slices of the heart.

The rate constants were obtained from the clearance curves as shown in Table 3 (n = 6). The values of C_1 and C_2 are expressed as a relative percentage. The rate constant of the first phase (k_1) was 0.249 ± 0.050/min (average half-life 2.8 min) in the myocardium without perfusion defect. The second phase (k_2) was 0.012 ± 0.004/min (average half-life 58 min) in the myocardium. The lung clearance

TABLE 2
Relative SPECT Count in Several Selected Acquisition Intervals (mean ± s.e.m.)

Interval used (min)	Acquisition time added (min)	Count rate in Myo	Count rate in Lung (% count/pixel/min)	Count rate in Liver	Ratio Myo/Lung	Ratio Myo/Liver
1– 2	1	100*	50 ± 8	81 ± 11	1.95 ± 0.48	2.07 ± 0.64
3– 6	3	70 ± 2	24 ± 2	109 ± 15	2.83 ± 0.42	0.85 ± 0.13
6– 9	3	54 ± 2	20 ± 2	134 ± 13	2.82 ± 0.26	0.51 ± 0.07
9–12	3	46 ± 2	18 ± 2	149 ± 20	2.55 ± 0.24	0.40 ± 0.06
11–21	10	39 ± 2	17 ± 1	150 ± 25	2.36 ± 0.19	0.35 ± 0.05

* The myocardial SPECT count in the second frame is standardized to 100%.

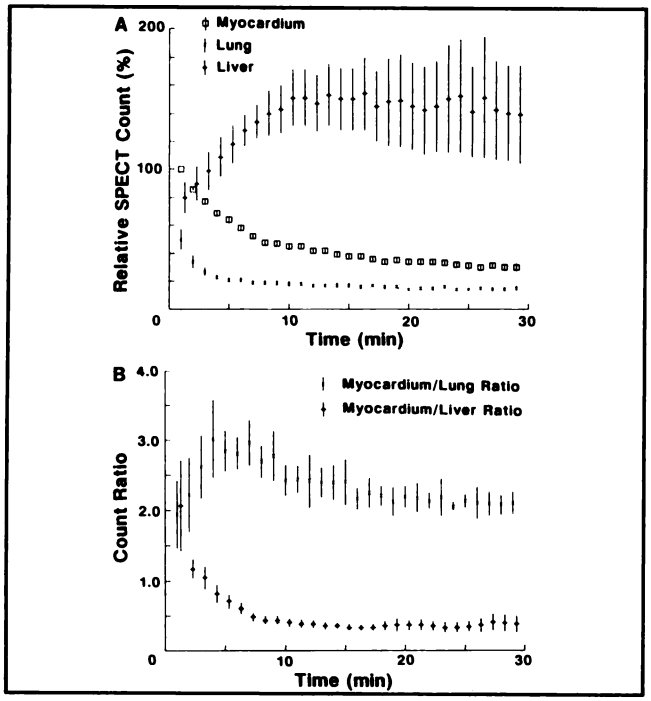

FIGURE 3. (A) Time-activity curves generated from ROIs on the myocardium (square), lung (cross), and liver (asterisk). The first data point that contains artifacts is excluded from the graph, and the second datapoint of the myocardium is standardized to 100%. Mean and s.e.m. are shown.
(B) Myocardium-to-lung (cross) and myocardium-to-liver (asterisk) ratios (mean and s.e.m.). The myocardium-to-lung ratio reached a peak around 5–8 min and gradually decreased thereafter, while the myocardium-to-liver ratio decreased rapidly till 9 min.

showed the clearance rate of 0.668 ± 0.113/min (average half-life 1.0 min) in k_1, followed by a slow component similar to that of myocardium.

DISCUSSION

Technetium-99m-SQ30217 (teboroxime), a neutral lipophilic technetium imaging agent, has been reported to be a promising radionuclide for scintigraphy from studies in animals. cultured cells, and humans (*2–13*). Favorable characteristics of SQ30217 include high initial myocardial uptake, rapid decrease in lung activity, good correlation with the myocardial blood flow as assessed by microsphere technique (*4,6,10*), and better physical property of ^{99m}Tc compared with that of ^{201}Tl. The rapid clearance can be an advantage, because rest-exercise studies can be repeated at short intervals. However, conversely, it can be a weakness when applying this radiopharmaceutical to SPECT studies. Accordingly, the dynamic changes of ^{99m}Tc-SQ30217 have been mainly evaluated by planar imaging (*4,7,12*). In this study, we used a triangular SPECT system that has both high sensitivity and high resolution (*14–17*). The acquisition time for a series of projection images can be significantly reduced using a three-detector SPECT system and continuous repetitive rotation acquisitions.

TABLE 3
Clearance of ^{99m}Tc-SQ30217 in Myocardium and Lung (mean ± s.e.m.)

Region (n = 6)	C_1 (%)	k_1 (/min)	C_2 (%)	k_2 (/min)
Myocardium	66 ± 3.1	0.249 ± 0.050	34 ± 3.1	0.012 ± 0.004
Lung	78 ± 2.7	0.668 ± 0.113	22 ± 2.7	0.013 ± 0.003

Dynamic SPECT Data Acquisition

To optimize SPECT studies with SQ30217 we fixed a method of continuous repetitive rotation acquisition. This method has several advantages. First, the SPECT data acquisition implicitly assumes that the accumulation pattern does not change during projection data acquisition. However, in radiopharmaceuticals which show rapid changes of distribution, relative activities in organs change significantly, resulting in artifacts after SPECT reconstruction. For example, in ^{99m}Tc-SQ30217, supposing the situation when data acquisition starts from the right anterior oblique (RAO) and the camera rotates anteriorly to the left posterior oblique (LPO), the RAO view has a relatively high myocardial uptake and low liver uptake, while the LPO view may show a decreased myocardial uptake and high overlapping liver uptake on the inferoapical wall. It does not seem reasonable to discard the phase of the highest myocardial activity to obtain a more stable phase at a later time, as shown in Figure 3, although the latter may have less artifact. The continuous repetitive acquisition also contains the rapidly changing phase; however, the difference in every projection is relatively small, and is averaged by the summation of the projection data. Therefore, the method described in this study may be an effective method for data acquisition. Second, the best timing of projection images for reconstruction can be selected after data acquisition. The increase of hepatic activity and the degree of its overlap to inferior and myocardial clearance may differ in each case. With this technique, the best timing of the initiation of data acquisition and possible total acquisition time can be arbitrarily changed. A series of acquisitions can be used to decide the best timing for SPECT, as well as to observe the dynamic changes of the tracer.

This type of dynamic acquisition requires a large memory size on the computer disk. However, if washout analysis is not required, only the projection images from the best interval may be added and stored. There is no practical problem if the disk is occupied temporarily.

The Best Timing for Data Acquisition

With regard to image quality and the overlap of the liver to the inferoapical wall, the superiority of early short-time acquisition to delayed data acquisition was evident in this study. Since the early myocardial uptake was high, only 3 min of data acquisition were needed for a good image. The superimposition of the inferior myocardial wall and liver could be avoided in all patients. On the other hand, in delayed imaging after 9 min, the inferior wall or apex

was obscured to some extent by the hepatic activity. Even if there was no significant overlap, the influence of Compton scatter from the hepatic activity was not negligible from the quantitative point of view. Thus, the possibility of early short-time data acquisition with a single-headed SPECT and 180° rotation should be further investigated as studied by Li et al. in dogs (*10*).

In myocardial scintigraphy at rest, this approach is recommended. The SPECT study can be finished within 10 min. However, in exercise study, the initiation of data acquisition just after intravenous injection seemed to be more difficult. Nevertheless, if the patient does not have severe symptoms at peak exercise, he can be moved to the SPECT couch in a few minutes. Performing the exercise study beside the SPECT machine, or leaving the ECG electrodes and infusion line in place after exercise, may facilitate the early start of the SPECT study. The factors causing the artifacts immediately after exercise, such as the changes in chamber size, respiratory movement, and "upward creep" (*18*) cannot be neglected, but their influence may be reduced by the continuous repetitive rotation acquisition with short intervals. However, since we do not have an experience of exercise ^{99m}Tc-SQ30217 study, this point also should be clarified with dynamic acquisition protocol.

Clearance of ^{99m}Tc-SQ30217

The half-life of the washout rate from the myocardium without defect was approximately 2.8 min in the first phase and 58 min in the second phase. These values are comparable to those obtained in planar imaging studies (*4,9*). Stewart et al. reported that the clearance of the rapid phase correlated with myocardial blood flow studied by SPECT in dogs (*19*). Therefore, both of rapid-sequence SPECT images and the best quality images from the appropriate intervals appear to be important in ^{99m}Tc-SQ30217 study. The continuous repetitive rotation acquisition and the reformatting of projection images as described in this study can contribute to the myocardial perfusion study using ^{99m}Tc-SQ30217.

In conclusion, the continuous repetitive rotation acquisition in SPECT study can be an effective method for radiopharmaceuticals that show rapid changes of distribution. When the technique was applied to ^{99m}Tc-SQ30217, the SPECT images within 9 min after injection showed superior image quality than those of the delayed SPECT images from the viewpoints of high myocardial uptake and less influence from the hepatic activity.

REFERENCES

1. Shelbert HR. Current status and prospects of new radionuclides and radiopharmaceuticals for cardiovascular nuclear medicine. *Semin Nucl Med* 1987;17:145–181.
2. Nunn AD, Treher EN, Feld T. Boronic acid adducts of technetium oxime complexes (BATOs). A new class of neutral complexes with myocardial imaging capabilities [Abstract]. *J Nucl Med* 1986;27:893.
3. Coleman RE, Maturi M, Nun AD, Eckelman WC, Juri PN, Cobb FR. Imaging of myocardial perfusion with ^{99m}Tc-SQ30217: dog and human studies [Abstract]. *J Nucl Med* 1986;27:893–894.
4. Narra RK, Feld T, Wedeking P, Matyas J, Nunn AD. SQ30217, A technetium-99m-labeled myocardial imaging agent which shows no interspecies differences in uptake [Abstract]. *J Nucl Med* 1986;27:1051–1052.
5. Maublant JC, Moins N, Renoux M, Gachon P. A comparison between Tl-201 and three Tc-99m-labeled myocardial blood flow imaging agents in cultured cardiac cells [Abstract]. *Clin Nucl Med* 1988;13(9S):p11.
6. Coleman RE, Maturi M, Nunn AD, Eckelmann WC. Myocardial perfusion: comparison of SQ30217, thallium-201, and microspheres in dogs [Abstract]. *J Nucl Med* 1987;28:1080.
7. Narra RK, Nunn AD, Kuczynski BL, Feld T, Wedeking P, Eckelman WC. A neutral technetium-99m complex for myocardial imaging. *J Nucl Med* 1989;30:1830–1837.
8. Meerdink DJ, Thurber M, Savage S, Leppo JA. Comparative myocardial extraction of two technetium-labeled boron oxime derivatives (SQ30,217, SQ32,014) and thallium [Abstract]. *J Nucl Med* 1988;29:972.
9. Johnson LL, Seldin DW, Muschel M, Smith K, Blood DK, Cannon PJ. Rest and exercise myocardial perfusion scans and clearance rates of SQ30217, a new technetium-99m perfusion imaging agent [Abstract]. *J Am Coll Cardiol* 1987;9(2 suppl A):138A.
10. Li QS, Solot G, Frank TL, Wagner HN Jr, Becker LC. Serial rest and dipyridamole tomographic myocardial perfusion studies with the rapidly clearing Tc-99m agent SQ30217. In: Schmidt HAE, Burragi GL, eds. *Nuclear medicine: trends and possibilities in nuclear medicine.* Stuttgart: Shattauer; 1989:243–246.
11. Seldin DW, Johnson LL, Muschel M, et al. Localization of myocardial perfusion defects on planar SQ 30,217 scans: comparison with thallium-201 scans and coronary anatomy [Abstract]. *J Nucl Med* 1987;28(suppl 4): 663.
12. Seldin DW, Johnson LL, Blood DK, et al. Myocardial perfusion imaging with technetium-99m SQ30217: comparison with thallium-201 and coronary anatomy. *J Nucl Med* 1989;30:312–319.
13. Zielonka JS, Bellinger R, Coleman RE, et al. Multicenter clinical trial of 99m-Tc-teboroxime (SQ 30,217; Cardiotec) as a myocardial perfusion agent. *J Nucl Med* 1989;30:1745.
14. Lim CB, Gottschalk S, Walker R. et al. Triangular SPECT system for 3-D total organ volume imaging: design concept and preliminary imaging results. *IEEE Trans Nucl Sci* 1985;NS-32(1):741–747.
15. Lim CB, Walker R, Pinkstaff C, et al. Triangular SPECT system for 3-D total organ volume imaging: performance results and dynamic imaging capability. *IEEE Trans Nucl Sci* 1986;NS-331(1):501–504.
16. Nakajima K, Taki J, Hisada K, et al. A three-headed SPECT system with high resolution and high sensitivity: application to myocardial imaging. *Jpn J Nucl Med* 1990;27:493–497.
17. Ichihara T. Development of a high-resolution SPECT system. *Toshiba Medical Review* 1990;33:29–35.
18. Friedman J, Van Train K, Maddahi J, et al. "Upward creep" of the heart: a frequent source of false-positive reversible defects on Tl-201 stress-redistribution SPECT [Abstract]. *J Nucl Med* 1986;27:899.
19. Stewart RE, Schwaiger M, Hutchins GD, et al. Myocardial clearance kinetics of technetium-99m-SQ30217: a marker of regional myocardial blood flow. *J Nucl Med* 1990;31:1183–1190.